

10587

NACA TN 4246

0066816



TECH LIBRARY KAFB, NM

NATIONAL ADVISORY COMMITTEE FOR AERONAUTICS

TECHNICAL NOTE 4246

FURTHER INVESTIGATION OF FATIGUE-CRACK PROPAGATION
IN ALUMINUM-ALLOY BOX BEAMS

By Herbert F. Hardrath and Herbert A. Leybold

Langley Aeronautical Laboratory
Langley Field, Va.



Washington

June 1958

AFMBC
LIBRARY



0066816

NATIONAL ADVISORY COMMITTEE FOR AERONAUTICS

TECHNICAL NOTE 4246

FURTHER INVESTIGATION OF FATIGUE-CRACK PROPAGATION

IN ALUMINUM-ALLOY BOX BEAMS

By Herbert F. Hardrath and Herbert A. Leybold

SUMMARY

Twenty-one box beams constructed according to nine designs were subjected to fatigue tests at one load level to study fatigue-crack propagation and accompanying stress redistribution. Six designs had stiffeners riveted to the skin, two had integrally stiffened covers, and one had stiffeners bonded to the skin. Specimens of each design were constructed of 7075 aluminum alloy. Additional specimens of some of the designs were constructed of 2024 aluminum alloy. The rate of crack propagation in specimens made of 7075 material was more rapid than that in equivalent specimens made of 2024 material. Specimens with bonded stringers had lower rates of crack growth than any other specimens tested. The most rapid rates of crack growth were found in specimens having the smallest total stringer area and in specimens with integrally stiffened covers.

INTRODUCTION

One of the important design features of current aircraft structures is the "fail-safe" characteristic. This feature is now receiving much more attention than it did in the past to eliminate the danger of catastrophic failures which might be caused by fatigue cracks or accidental damage.

The National Advisory Committee for Aeronautics is currently conducting several investigations of the fail-safe characteristics of typical structural parts. Preliminary results of that part of this study which applies particularly to the study of rate of fatigue-crack propagation in wing structures have been presented in reference 1. The results presented in that work indicated that the mode of connecting stringers to the skin had an important influence on the rate of crack propagation. Additional tests have been performed to investigate this influence in more detail.

Two designs of box beams with rivet spacings one-half and twice that used in reference 1 and one design with stringers bonded to the skin were tested. In each of these designs the ratio of stringer area A_t to skin area A_s was about 1.

Some current airplane wings have lower values of A_t/A_s than that used in the riveted and bonded beams. In order to study configurations representative of these wings, another series of tests was conducted on specimens in which the amount of stringer material was reduced by one-half. Three designs were tested to study various ways of arranging the smaller stringer area.

One design of beams with integrally stiffened extruded covers was tested for comparison with previously reported results on covers machined from a plate. One specimen with a cover machined from a plate was tested to duplicate earlier tests.

Some of the data presented in the present paper have been discussed in a preliminary way in reference 2 together with preliminary results of several other investigations.

APPARATUS AND TESTS

Specimens

In general, the test beams were similar to those discussed in reference 1. Each was 20 inches wide and 8 feet long. They were supported at the ends and were loaded at two spanwise stations to provide a constant-moment section 2 feet long at the center.

The primary load-carrying elements of a given specimen were all made of the same basic aluminum alloy; that is, in 2024 beams all sheet material in the covers and shear webs was 2024-T3 and all extrusions were 2024-T4, and in 7075 beams all elements were 7075-T6. For brevity, all temper designations are omitted in the following discussion. Unless otherwise noted, all rivets were made of 2117-T3 aluminum alloy and were 3/16 inch in diameter with brazier heads. All stringers were extruded angles.

Each beam had an oblong hole in the middle of the cover to initiate cracks there. This hole was made by drilling two $\frac{1}{4}$ -inch-diameter holes, one on each side of the longitudinal center line of the beam, and removing the material between these holes. The transverse cross section containing this oblong hole is referred to as the critical section of the beam.

The code designation used in reference 1 to facilitate reference to specific beams was extended to cover all the beams tested in this investigation. This designation (for instance, 6B-1) is explained as follows: the first digit is a number corresponding to the design number which is described in succeeding paragraphs, the letter identifies the alloy from which the beam was built (A for 2024 and B for 7075), and the last digit is a number designating the first, second, third, or fourth specimen of a given design and material. In the example, specimen 6B-1 represents the first beam constructed of 7075 aluminum alloy according to design 6.

The distinguishing features of the various designs tested in the present investigation are summarized in table I, in figure 1, and in the description which follows. Details of designs tested in the previous investigation are also summarized in table I.

Design 2: One specimen (2B-3) was constructed of 7075 material with the same geometry as that for the beams of design 2 in reference 1 except that no rivets were in the critical section. Eight stringers ($\frac{1}{16}$ by 1 by 1 inch) were riveted to the skin with a $1\frac{1}{2}$ -inch pitch.

Design 3: Eight stringers ($\frac{1}{16}$ by 1 by 1 inch) were bonded to the skin with a two-component ethoxyline resin (liquid form) rather than a one-component ethoxyline resin (stick form) used in beams reported in reference 1. The cross section of this design is identical to that of design 2. Two beams (3B-3 and 3B-4) were built of 7075 aluminum alloy.

Design 4: One specimen (4B-3) of 7075 aluminum alloy had a cover with integral stiffeners machined from a plate. The radius of the fillet between skin and stiffeners was approximately $1/8$ inch.

Design 5: Beams built according to design 5 had integrally stiffened extruded covers. In order to make the geometry similar to that of covers machined from a plate, the extrusions were modified as shown in figure 1. After machining, the thickness of the skin between stiffeners was 0.081 inch, the stiffener thickness was 0.102 inch, the stiffener depth (including the skin thickness) was 0.75 inch, and the fillet radius was approximately $1/8$ inch. The cover was not cambered in this type of construction. Two beams were built of each of the alloys, 2024 and 7075 (specimens 5A-1, 5A-2, 5B-1, and 5B-2).

Design 6: Beams built according to design 6 were identical in cross section to those of design 2 but had a 3-inch rivet pitch in the stringers in the carry-through bay instead of a $1\frac{1}{2}$ -inch pitch. Two beams

were built of 2024 aluminum alloy (6A-1 and 6A-2) and two of 7075 aluminum alloy (6B-1 and 6B-2) with the rivets placed in such a way that no rivets fell in the critical section. One additional 7075 beam (6B-3) was constructed with rivets in the critical section.

Design 7: Beams built according to design 7 were identical in cross section to those of design 2 except that they had a $\frac{3}{4}$ -inch rivet pitch in the stringers in the carry-through bay instead of a $1\frac{1}{2}$ -inch pitch. In this design, one rivet in each stringer was in the critical section. Again, two beams were constructed of each of the two alloys (specimens 7A-1, 7A-2, 7B-1, and 7B-2).

Design 8: Beams built according to design 8 were similar to those of design 2 except that there were only four longitudinal stringers rather than eight in each tension cover. In this design, one specimen (8B-2) was constructed with no rivets in the critical section and one specimen (8B-1), with one rivet in each stringer in the critical section. Both beams were built of 7075 aluminum alloy. This design and the two following are the designs having the lower value of the ratio of stringer area to skin area A_t/A_s .

Design 9: The beam built according to design 9 (9B-1) was similar to those of design 2 except that the eight longitudinal stringers were $\frac{1}{16}$ by $\frac{1}{2}$ by $\frac{1}{2}$ inch rather than $\frac{1}{16}$ by 1 by 1 inch. No rivets were in the critical section. Rivets with $\frac{1}{8}$ -inch diameter were used to connect the stringers to the skin. One beam was built of 7075 aluminum alloy.

Design 10: The beam built according to design 10 (10B-1) was the same as that of design 9 except that $\frac{5}{32}$ -inch rivets were used and one rivet in each stringer was in the critical section. This beam was constructed by removing the tension cover of specimen 9B-1 after testing and placing a new 7075 cover on the same box.

Equipment and Procedure

The equipment and procedure used were identical to those described in reference 1. All specimens were tested at a stress of 13 ± 6.5 ksi as indicated by resistance wire strain gages on the skin at the critical section. This stress level was chosen in reference 1 to be representative

of 1g stresses used in practice and to produce failure in a reasonable time. The testing machine was adjusted as needed to maintain loads within ± 3 percent of initial values. These loads were measured by resistance wire strain gages on the struts supporting the specimens.

Strain-gage readings were taken at intervals during the test to study the redistribution of stresses as the crack progressed across the cover. Strain gages for this purpose were applied to the skin at 1-inch intervals and one on each stringer, all at the critical section.

TEST RESULTS

Crack Initiation

In general, cracks developed at the hole in the center of the tension cover and then propagated across the beam at this cross section. Two exceptions to this trend are described in subsequent sections.

The number of cycles of load applied to each beam to produce a visible crack is indicated by the shaded areas of the bar graph in figure 2. The differences seen are probably not significant, compared with normal scatter, in spite of the fact that two alloys in three basic forms (sheet, extrusion, and plate) are involved.

The unshaded bars in figure 2 indicate the additional cycles of load required to propagate cracks through 20 percent of the gross tension cross-sectional area. At this point in the tests the cracks were growing so rapidly that final failure was imminent. For comparison, the dotted line (taken from ref. 1) indicates the life which might be expected for final failure of simple specimens containing the same effective stress concentration as that of the oblong hole and subjected to the same stresses as were applied to these beams. Predictions made for simple specimens appear to be optimistic when applied to lives of the beams tested in the present investigation.

Crack Propagation

The crack-propagation histories for each of the beams tested are shown in figures 3 to 7 as the percentage of the gross tension cross-sectional area lost plotted against the number of load cycles applied after crack initiation. The net area had been used in reference 1, but the use of gross area appears more consistent when comparing configurations which may or may not contain rivet holes in the critical cross section and when comparing residual static strengths as was done in

reference 2. The interpretation of results is not affected significantly by this change. The initial point on each curve is plotted at a value of area lost of approximately 1 percent to account for the hole present before the crack initiates. The area removed by each rivet hole was deducted when the crack reached that hole. All curves are plotted to the same scale to aid in making comparisons between the various designs tested. Data from reference 1 are repeated in some of the figures to facilitate comparison with present data.

In general, the fatigue cracks propagated in a manner similar to that discussed in reference 1. Crack propagation was always more rapid in 7075 beams than in 2024 beams with the same configuration. Fatigue cracks grew slowly through the first panel and more rapidly in later stages of the test. Crack growth was always rapid after one or more stringers failed. (Unless otherwise noted, the terms crack growth and rate of crack propagation will refer to percentage of gross tension cross-sectional area lost.) The circular symbols on the curves (figs. 3, 5, 6, and 7) indicate the amount of gross tension cross-sectional area that had failed just after a stringer failed. In some cases, two stringers failed almost simultaneously; therefore, the number 2 beside circular symbols on some curves indicates that two stringers failed simultaneously at that stage of the test.

Behavior peculiar to each particular design is discussed in the following sections.

Design 2.- The crack in specimen 2B-3 grew steadily across the critical section as indicated by the crack-propagation curve in figure 3. Since no rivet holes were in the path of the crack to interrupt crack growth, the propagation curve is very much like that for specimen 2B-1 (ref. 1), in which the crack veered off the rivet line on one side of the specimen.

Design 3.- The behavior of beams with bonded covers (3B-3 and 3B-4) was essentially the same as that of 7075 beams of design 3 reported previously (specimens 3B-1 and 3B-2 in ref. 1). The crack-propagation curves for all four beams are shown in figure 4. As mentioned previously, a two-component ethoxyline resin (liquid form) was used in specimens 3B-3 and 3B-4 instead of the one-component ethoxyline resin (stick form) used in specimens 3B-1 and 3B-2. Results from tests of simple specimens (fig. 8) bonded with both types of adhesive are presented in table II. The shear strengths listed in the table indicate that when good bonds are achieved, as was the case in the simple specimens, the average shear strength was essentially the same for all combinations of alloy and adhesive. Inspection of the bonds in the 7075 box beams after testing revealed that these bonds also were consistently good and, therefore, the uniform behavior was to be expected.

Specimen 3B-4 developed two cracks in abnormal locations. These cracks, $8\frac{1}{4}$ and $18\frac{3}{4}$ inches from the critical section, were discovered after 139,200 cycles of load were applied. At that time the crack at the critical section had progressed approximately 11 inches. The crack nearest the critical section was approximately $2\frac{1}{2}$ inches long through a flange rivet. The flange angle and about 2 inches of the web were also cracked. The crack farthest from the critical section was about $1\frac{3}{4}$ inches long through a flange rivet. The test was discontinued at this point. Specimen 3B-4 had the lowest average rate of crack propagation shown in figure 4, but differences are probably not significant. The extra cracks, therefore, had little effect on the results.

Design 4.- The single 7075 beam with a cover machined from a plate (4B-3) was tested to study crack propagation in beams constructed according to design 4 without the special 0.003-radius notch used in testing specimen 4B-2 of reference 1. The crack-propagation curve for this beam is shown in figure 5. Also plotted in this figure are curves for the beams of design 4 reported in reference 1. The curve for specimen 4B-3 is very close to that for specimen 4B-2. Stiffeners failed soon after the crack had grown through adjacent panels.

Design 5.- Crack-propagation curves for beams with extruded covers (design 5) are also shown in figure 5. In each case, the rate of propagation was slightly less than that in beams having covers machined from a plate (design 4) of the same alloy. As in covers machined from a plate, the stringers failed shortly after the fatigue crack had grown through the adjacent panel.

Design 6.- The crack-propagation curves for specimens with 3-inch rivet pitch (design 6) are shown in figures 3 and 6 for 7075 and 2024 aluminum alloys, respectively. Other curves in each of these figures are for designs 2 and 7 which have rivets spaced $1\frac{1}{2}$ inches and $\frac{3}{4}$ inch apart, respectively. The curves for specimens 6B-1 and 6B-2 indicate more rapid crack growth in this design than in either of the other two. Since no rivet holes occurred in the critical section, there was no interruption of crack growth in the skin. No cracks initiated in the stringers before the crack had grown through practically the entire width of the skin at the critical section. On the other hand, specimen 6B-3 had rivets in its critical section. Consequently, crack propagation was interrupted by rivet holes, and the number of cycles of load required to propagate the crack through, for example, 20 percent of the

material, was more than doubled. No stringers had failed when the crack in the skin reached the flanges.

Design 7.- The curves for specimens built according to design 7 (figs. 3 and 6) indicate crack growth was practically the same as in specimens built according to design 2. However, the failure of the first stringer occurred much earlier in these tests than in tests of specimens built according to design 2. In specimen 7B-1 the crack grew to the first rivet on each side of the center hole, but then veered off the rivet line and continued along a line between rivet rows across two panels on each side of the beam. The resulting rate of crack propagation was somewhat greater than that which occurred in specimen 7B-2 (fig. 3), but the difference is small compared with the difference between curves for specimens 7A-1 and 7A-2 (fig. 6). The test conditions for the latter two beams were as nearly identical to each other as was possible.

Specimen 7B-2 developed a crack at the critical section in 51,600 cycles. At 95,500 cycles, a crack 4 inches long was found in the cover at the support station 12 inches from the critical section. The crack apparently grew from a rivet hole in the flange. This crack was patched by use of a fiber-glass technique described in reference 3. The test was resumed and continued until four panels and two stringers had failed at the critical section.

Design 8.- Crack propagation in beams with only four stringers (design 8) was more rapid than in any other design tested (fig. 7). In general, the cracks grew almost completely across the skin before a stringer failed. In specimen 8B-2 no rivets occurred in the critical section, accounting for the somewhat faster crack growth in 8B-2 than in 8B-1.

Design 9.- Crack growth in specimen 9B-1, which had the smallest rivets used in these specimens, was accompanied by shear failure in the rivets. Since no rivets occurred in the critical section, crack propagation in the sheet was rapid (fig. 7). No stringers failed before the crack had grown completely across the skin.

Design 10.- Using larger rivets and locating them in the critical section resulted in somewhat slower crack propagation in this beam (10B-1) than in specimen 9B-1 (fig. 7). One stringer failed when the crack in the skin had grown to 60 percent of the width of the beam.

Stresses

In general, the results of stress surveys made in each of the beams during the tests were similar to those reported in reference 1. The

stress at a given station increased markedly as the crack approached this station. The stress in a given stringer continued to rise until failure of that stringer occurred.

The increase in stringer stress ΔS at maximum load is shown in figure 9 for one beam in each design in which stringers were either riveted or bonded to the skins. The top plot of the figure shows the increase in stress in one of the two middle stringers in one specimen of each of designs 2, 3, 6, and 7. These beams are identical in cross section and in material of construction but vary in mode of connecting stringers to the skin. The bonded stringers had the lowest increase in stress because of the peeling back of the bond as the crack grew through the skin. The stress increase in riveted construction was greatest in beams with closest rivet spacing and least in beams with rivets spaced farther apart. Apparently, stringers with closely spaced rivets more effectively assumed forces previously carried by the sheet. The sudden increase in stringer stress in specimens built according to design 2 was caused by failure of the other middle stringer.

The bottom plot of figure 9 shows the increase in stress in one of the middle stringers in beams constructed with the lower value of A_t/A_s . The curve for design 2 is repeated for comparison. Of the three designs with the lower value of A_t/A_s , design 9 (eight stringers $\frac{1}{16}$ by $\frac{1}{2}$ by $\frac{1}{2}$ inch, $\frac{1}{8}$ -inch-diameter rivets) had the least increase in stringer stress. This was undoubtedly the result of failure of rivets as the crack grew across the cover. The stringers in specimens constructed according to design 8 (four stringers $\frac{1}{16}$ by 1 by 1 inch) and design 10 (eight stringers $\frac{1}{16}$ by $\frac{1}{2}$ by $\frac{1}{2}$ inch, $\frac{5}{32}$ -inch-diameter rivets) experienced a significantly greater increase in stress.

The greatest increase in stress occurred in the specimen constructed according to design 10. The increase in stringer stress in this specimen approaches twice the increase observed in specimens built according to design 2 up to the time that a stringer failed. These two designs had essentially the same geometry except for stringer size. Since the stringers in design 10 are half the size of those in design 2, a doubling of the increase in stringer stress is about what is to be expected.

In general, the increase in stringer stress for a given design was insensitive to location of the rivets with respect to the critical section.

DISCUSSION

The results of tests of specimens built according to designs 2 to 7 indicate several consistent trends in fatigue crack behavior as affected by the mode of connecting stringers to the skin.

Cracks always grew faster in the 7075 specimens than in the 2024 specimens with the same geometry.

In integrally stiffened covers a crack, once started, grew steadily until it reached the flanges of the beam. Thus, integral stiffeners had little effect on crack growth. The difference between rates of growth in extruded covers and in covers machined from a plate was small, but extruded covers had the lower rate, possibly because of the slightly heavier stringers used. The use of artificial crack stoppers is probably necessary to control crack growth in integrally stiffened wings. "Board" construction (ref. 4), in which the extruded cover is made up of several units side by side, is being used in some current aircraft. The type of beams used in this investigation is probably too narrow to use to investigate adequacy of this or other methods quantitatively.

Tests of beams with identical configurations except for rivet pitch (designs 2, 6, and 7) and with cracks growing in a cross section containing rivet holes indicate a somewhat more rapid rate of crack propagation in beams with greatest rivet pitch (design 6). This rapid rate of crack propagation is probably the result of less effective transfer of forces to the stringers in beams with greater rivet pitch. However, the differences in behavior due to rivet pitch are much less than differences in behavior due to the presence or the absence of rivet holes in the critical section. (See fig. 3.) Crack growth was temporarily stopped each time a crack reached a rivet hole and a new crack had to be initiated before additional propagation could take place. However, when the crack veered off the rivet line, as happened in specimen 2B-1 (ref. 1), crack growth was essentially as rapid as in specimen 2B-3 which had no rivets in the critical section. Thus, cracks cannot be depended upon to grow along lines least favorable to rapid crack growth.

Crack growth was much more rapid in beams with the lower value of A_t/A_s (designs 8, 9, and 10) than in beams with a value of A_t/A_s of approximately 1. Of the specimens with a low value of A_t/A_s , the specimens with only four stringers ($\frac{1}{16}$ by 1 by 1 inch, design 8) had the fastest rate of crack growth observed in these tests. The use of eight stringers ($\frac{1}{16}$ by $\frac{1}{2}$ by $\frac{1}{2}$ inch) in design 10 produced better crack-propagation

characteristics than was observed in design 8. This is due, in part, to the presence of more rivet holes in the critical section and, in part, to the more effective transfer of forces to stringers in design 10.

Bonded connections between skin and stringers appear to control rapid crack growth in the skin without introducing excessive stresses in the stringers. The absence of rivet holes in stringers makes these stringers even more immune to failure than in riveted construction. In spite of the fact that the crack grew through the skin without interruption by rivets, crack growth in the skin alone was significantly slower than in other types of construction. However, results are critically dependent upon the quality of the bond (ref. 1).

CONCLUDING REMARKS

The rate of fatigue-crack propagation in the covers of several configurations of built-up box-beam structures has been investigated. All cracks were grown at the same stress level in the constant-moment section of each of the beams. Cracks always grew more rapidly in 7075 specimens than in 2024 specimens constructed with the same configuration. Closely spaced rivets in the stringers produced lower rates of crack propagation than did rivets spaced farther apart. However, this difference was considerably less than that obtained by having rivets placed either in or not in the path of the fatigue crack. A reduction in area of stringers relative to the area of the skin resulted in much faster rates of crack growth. Cracks grew very rapidly through integrally stiffened covers because no barriers to crack growth were present. On the other hand, bonded covers, which also had no rivet holes in the critical section, had the slowest crack growth observed in these tests.

The observations listed are limited to cracks initiating in the skin and growing through a constant-moment section of built-up box beams. The behavior of cracks starting in stringers or flanges has not been studied, and no results are presented for cracks growing in sections of a box where a shear force is present. Conceivably, a shear force could have an important modifying influence on the results. Bonded construction, particularly, would be subjected to additional forces which might tend to decrease the effectiveness of the connections.

Langley Aeronautical Laboratory,
National Advisory Committee for Aeronautics,
Langley Field, Va., February 5, 1958.

REFERENCES

1. Hardrath, Herbert F., Leybold, Herbert A., Landers, Charles B., and Hauschild, Louis W.: Fatigue-Crack Propagation in Aluminum-Alloy Box Beams. NACA TN 3856, 1956.
2. Hardrath, Herbert F., and Whaley, Richard E.: Fatigue-Crack Propagation and Residual Static Strength of Built-Up Structures. NACA TN 4012, 1957.
3. McGuigan, M. J., Jr., Bryan, D. F., and Whaley, R. E.: Fatigue Investigation of Full-Scale Transport-Airplane Wings - Summary of Constant-Amplitude Tests Through 1953. NACA TN 3190, 1954.
4. Spaulding, E. H.: Observations on the Design of Fatigue-Resistant and 'Fail Safe' Aircraft Structures. Proc. Int. Conf. on Fatigue of Metals (London and New York), Inst. Mech. Eng. and A.S.M.E., 1956, pp. 628-640.

TABLE I

SUMMARY OF DISTINGUISHING FEATURES IN TEST BEAMS

Design	Material	Width, in.	Skin thickness, in.	Number of stringers	Size of stringers, in.	Stringer connection	Rivet pitch, in.	Rivets on or off critical section	Number tested	Report
1	2024 7075	12	0.051	4	$\frac{1}{16} \times 1 \times 1$	3/16-in. rivet	3/4	On	3 2	Ref. 1
2	2024 7075 7075	20	.051	8	$\frac{1}{16} \times 1 \times 1$	3/16-in. rivet	$1\frac{1}{2}$	On On Off	2 2 1	Ref. 1 Ref. 1 Present
3	2024 7075	20	.051	8	$\frac{1}{16} \times 1 \times 1$	One-component ethoxyline resin (stick form)			3 2	Ref. 1 Ref. 1
	7075	20	.051	8	$\frac{1}{16} \times 1 \times 1$	Two-component ethoxyline resin (liquid form)			2	Present
4	2024 7075 7075	20	.081	8	0.094 x 0.67	Integrally stiffened, machined			2 2 1	Ref. 1 Ref. 1 Present
5	2024 7075	20	.081	8	0.102 x 0.67	Integrally stiffened, extruded			2 2	Present
6	2024 7075 7075	20	.051	8	$\frac{1}{16} \times 1 \times 1$	3/16-in. rivet	3	Off Off On	2 2 1	Present
7	2024 7075	20	.051	8	$\frac{1}{16} \times 1 \times 1$	3/16-in. rivet	3/4	On On	2 2	Present
8	7075	20	.051	4	$\frac{1}{16} \times 1 \times 1$	3/16-in. rivet	$1\frac{1}{2}$	On Off	1 1	Present
9	7075	20	.051	8	$\frac{1}{16} \times \frac{1}{2} \times \frac{1}{2}$	1/8-in. rivet	$1\frac{1}{2}$	Off	1	Present
10	7075	20	.051	8	$\frac{1}{16} \times \frac{1}{2} \times \frac{1}{2}$	5/32-in. rivet	$1\frac{1}{2}$	On	1	Present

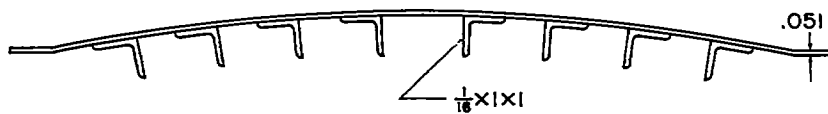
NACA TN 4246

TABLE II

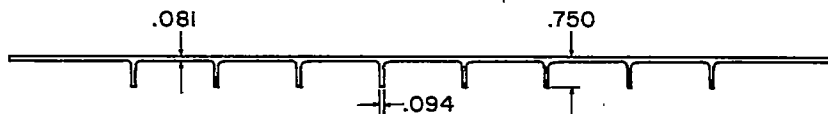
EVALUATION OF JOINTS BONDED WITH
 ETHOXYLINE-RESIN ADHESIVES

Adhesive	Aluminum alloy	Shear strength, ksi	Average shear strength, ksi
One-component ethoxyline resin (stick form)	2024	5.00 5.90 6.14	5.68
	7075	4.99 6.51 6.21	5.90
Two-component ethoxyline resin (liquid form)	2024	5.89 5.95 6.02	5.95
	7075	6.11 6.00 6.09	6.07

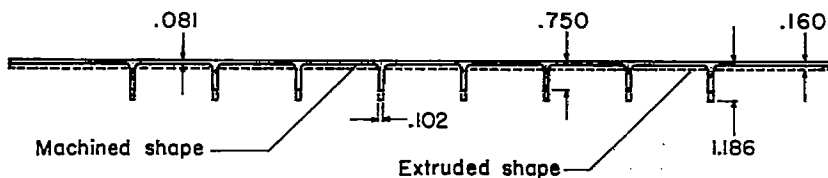
DESIGN 2,3,6,8,7



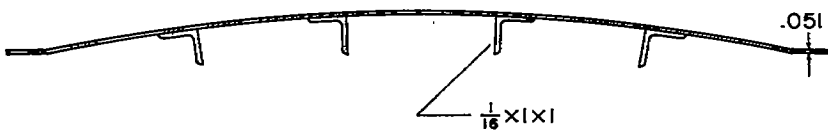
DESIGN 4



DESIGN 5



DESIGN 8



DESIGN 9 & 10

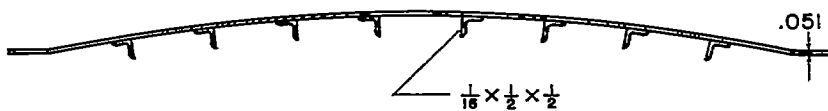


Figure 1.- Cover configurations. All dimensions are in inches.

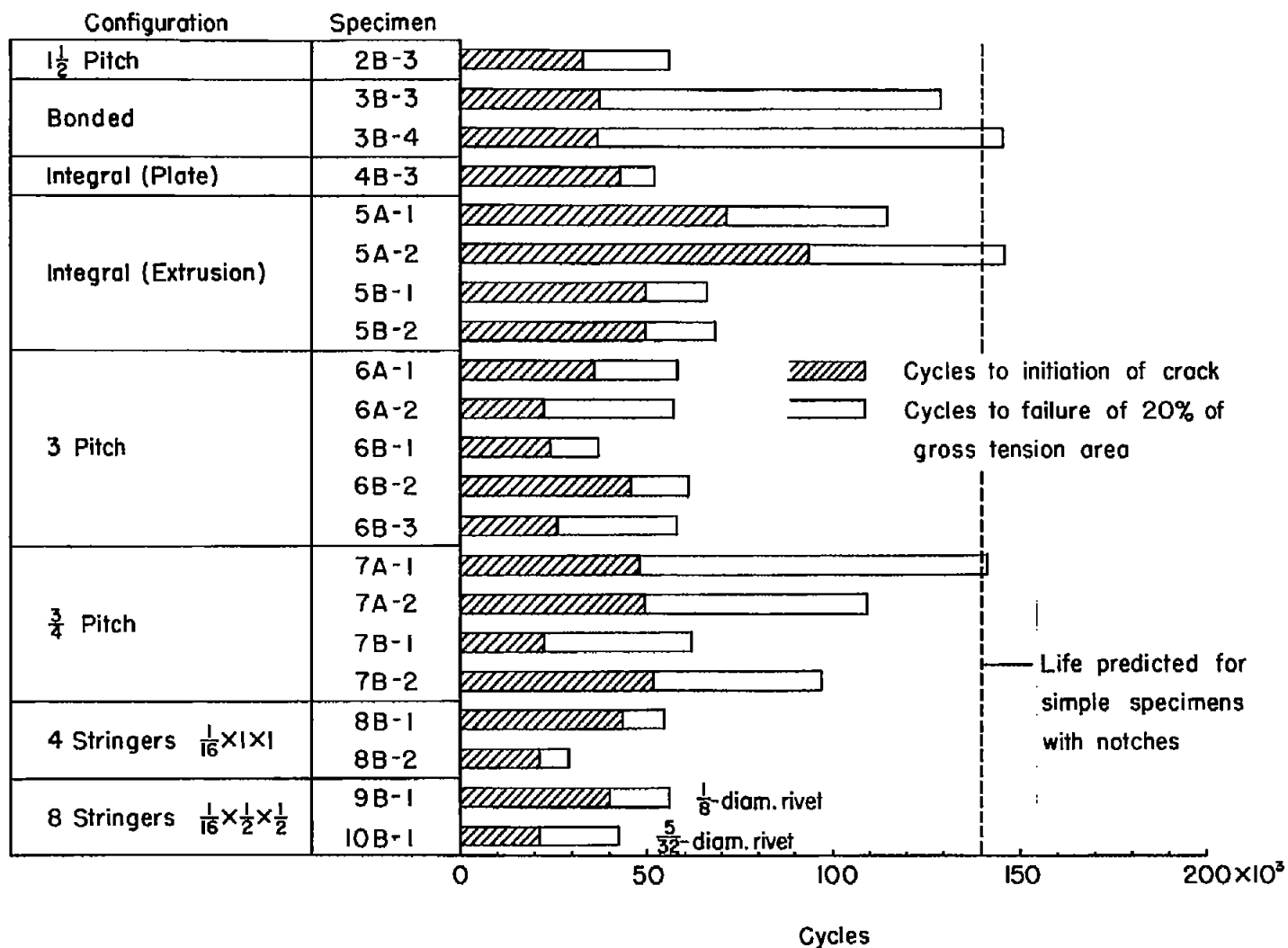


Figure 2.- Cycles required to initiate and to propagate cracks through 20 percent of the gross tension cross section in box beams. All dimensions are in inches.

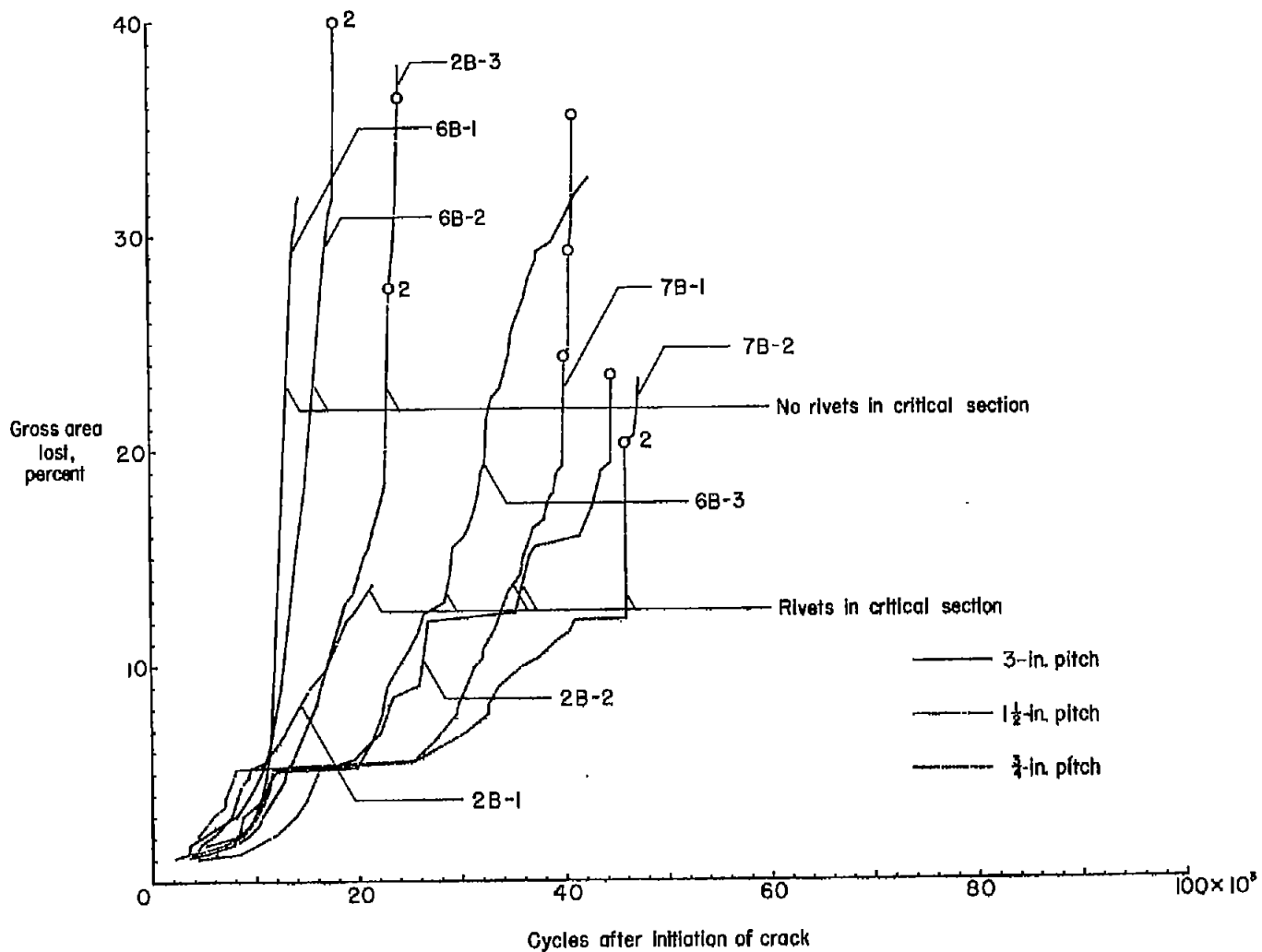


Figure 3.- Crack propagation in riveted specimens of 7075 aluminum alloy with $A_t/A_B = 1$. Data for specimens 2B-1 and 2B-2 are from reference 1. Circles indicate amount of material failed after stringer failure. Number 2 beside the circles indicates two stringers failed simultaneously.

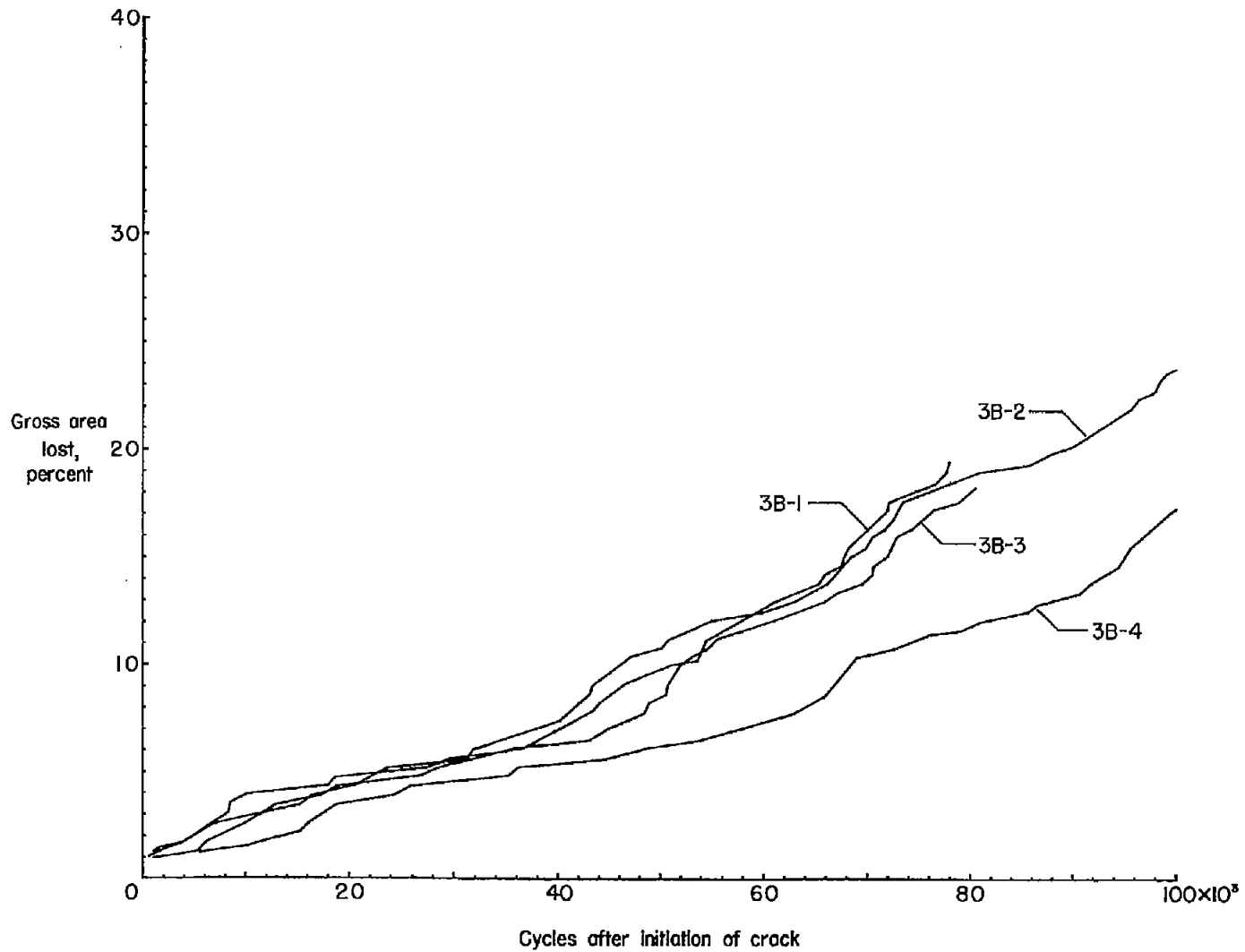


Figure 4.- Crack propagation in bonded specimens of 7075 aluminum alloy. Data for specimens 3B-1 and 3B-2 are from reference 1.

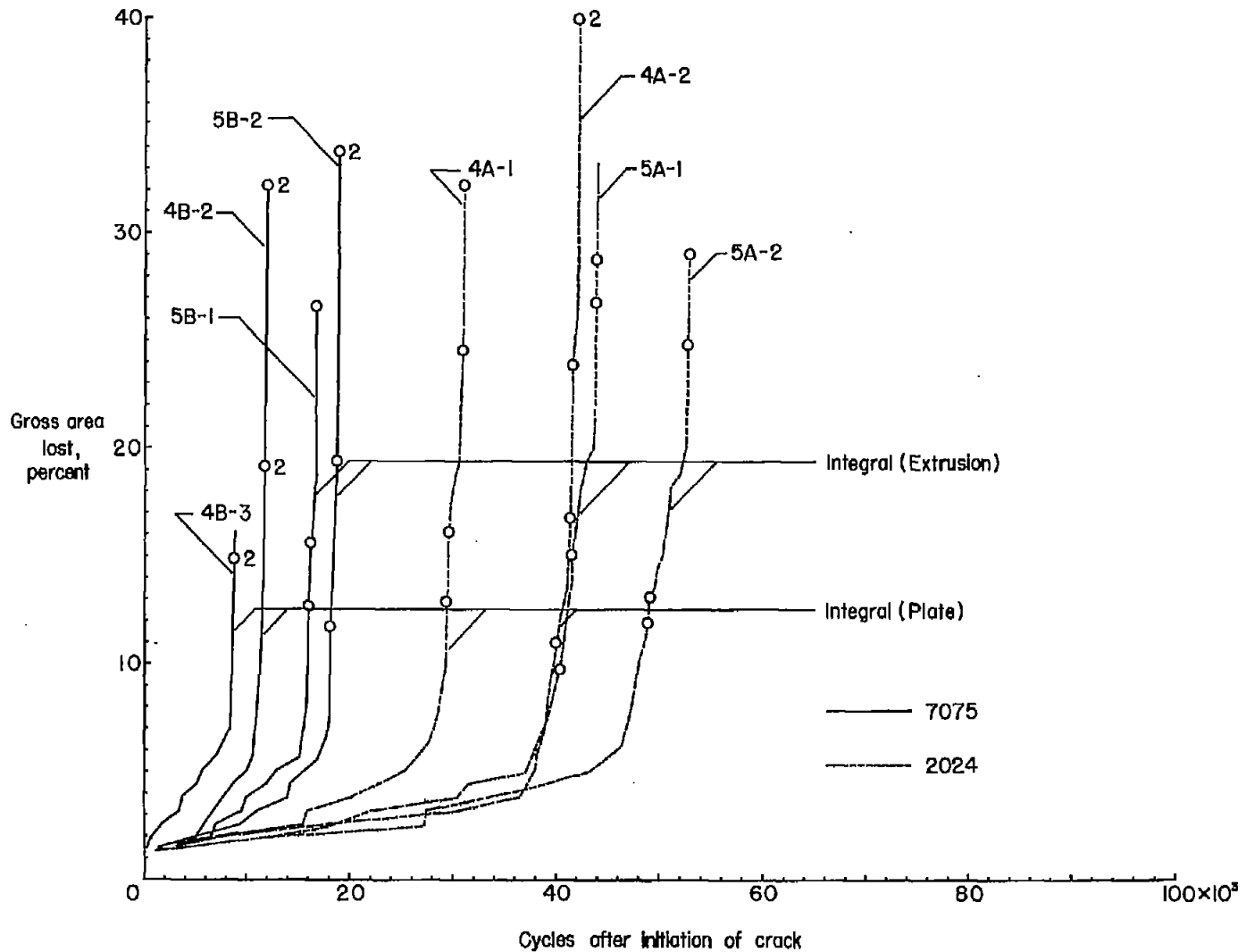


Figure 5.- Crack propagation in integrally stiffened specimens. Data for specimens 4A-1, 4A-2, and 4B-2 are from reference 1. Circles indicate amount of material failed after stringer failure. Number 2 beside circles indicates two stringers failed simultaneously.

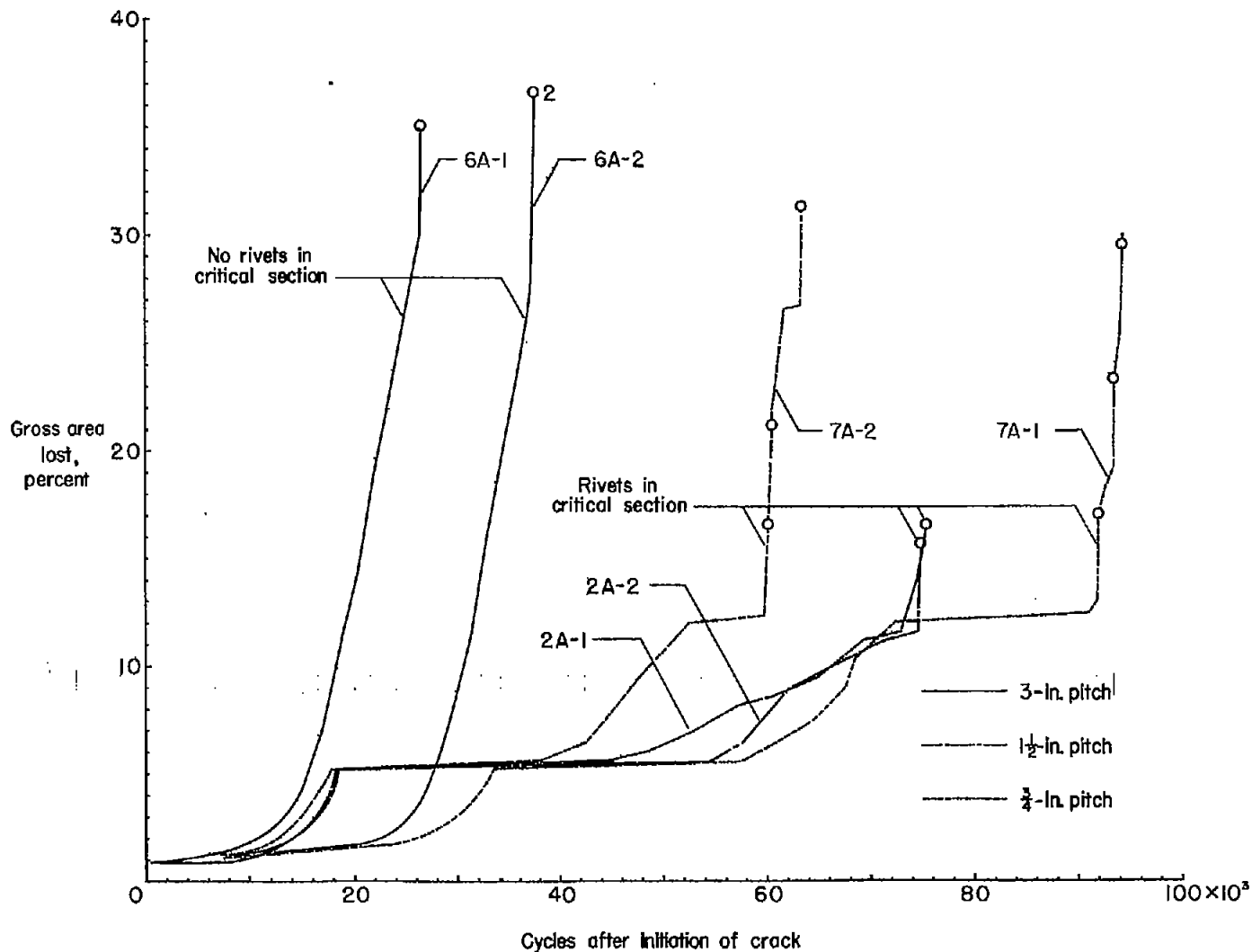


Figure 6.- Crack propagation in riveted specimens of 2024 aluminum alloy with $A_t/A_S = 1$. Data for specimens 2A-1 and 2A-2 are from reference 1. Circles indicate amount of material failed after stringer failure. Number 2 beside circles indicates two stringers failed simultaneously.

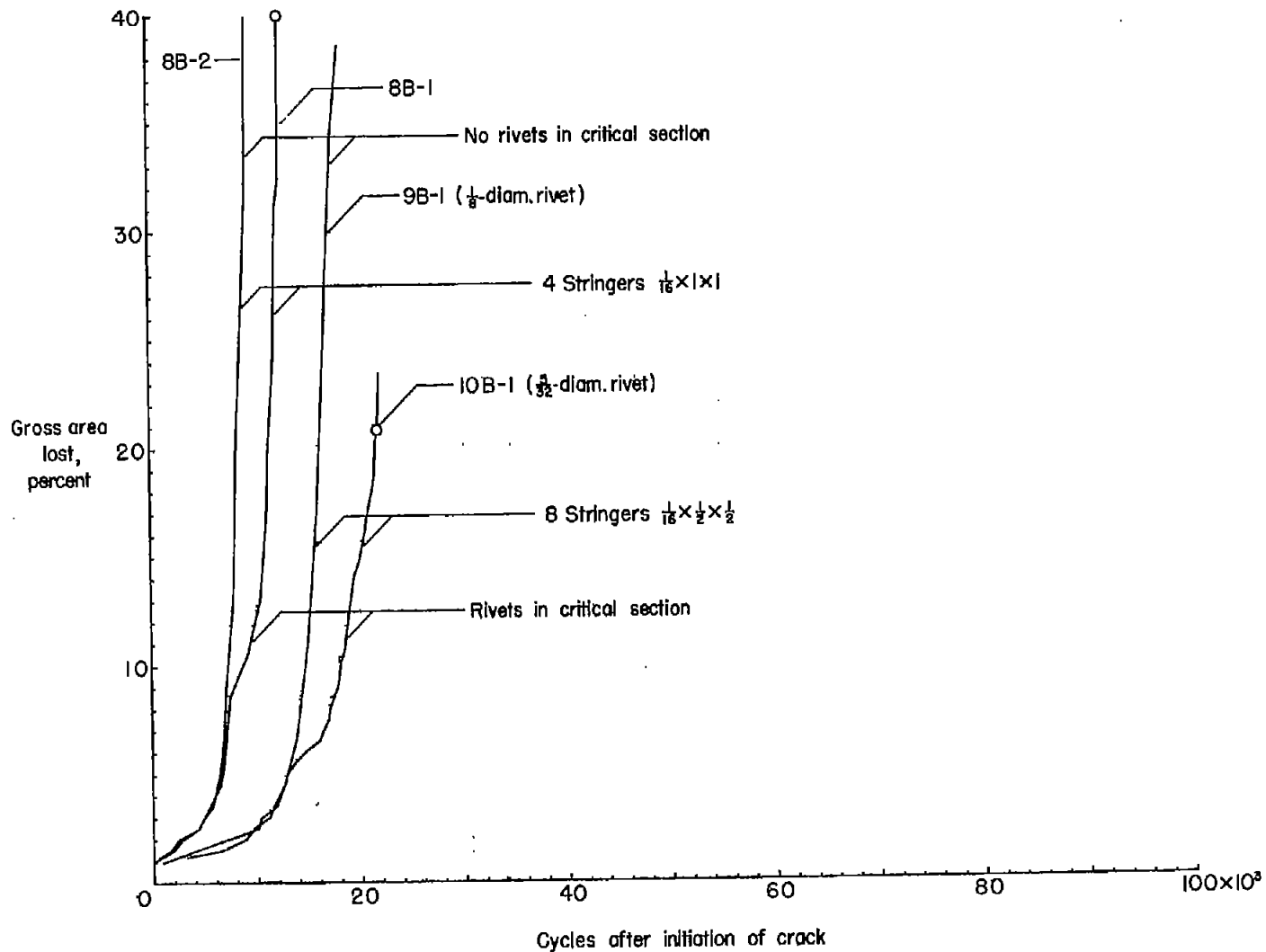


Figure 7.- Crack propagation in riveted specimens of 7075 aluminum alloy with $\frac{A_t}{A_s} = \frac{1}{2}$. Circles indicate amount of material failed after stringer failure. All dimensions are in inches.

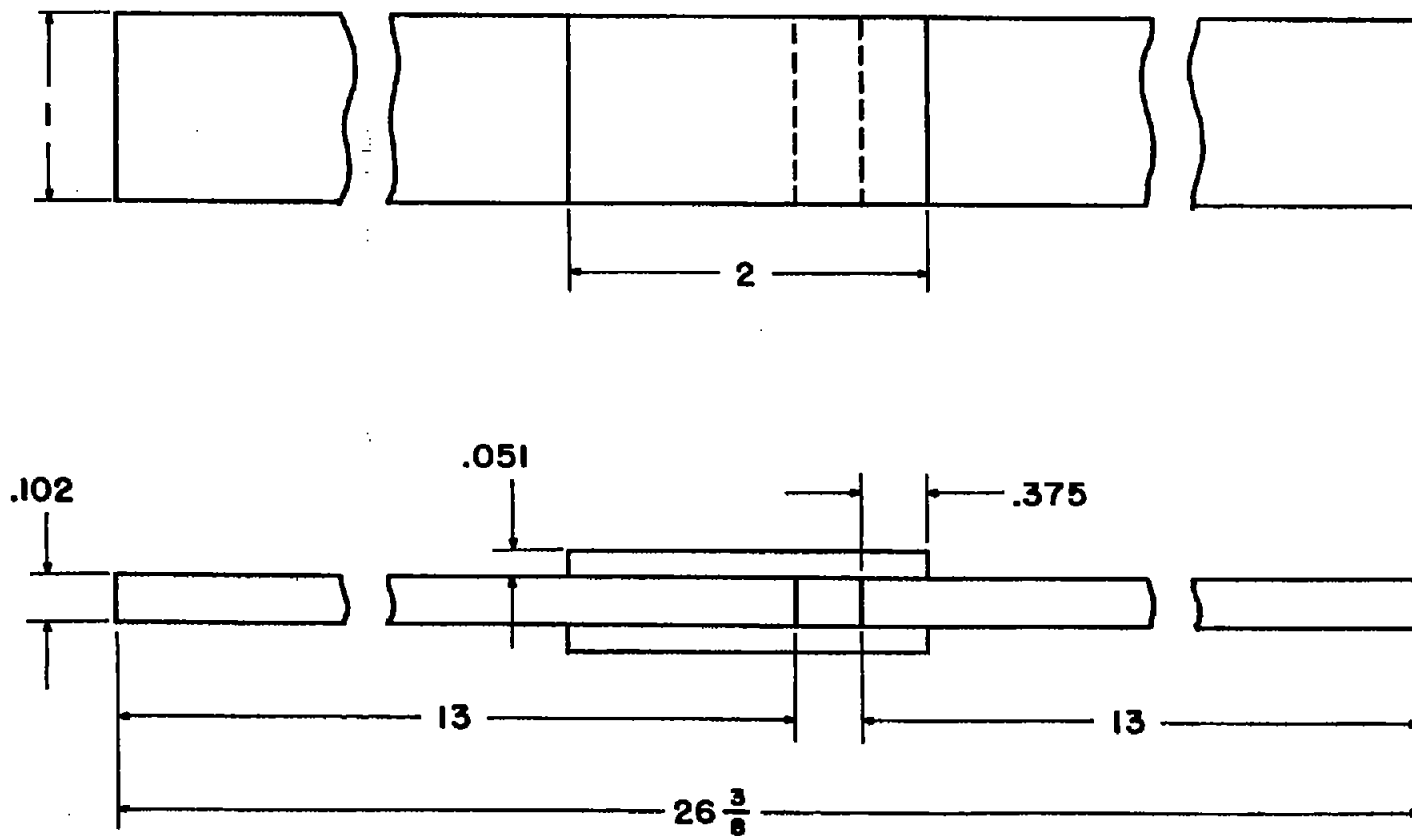


Figure 8.- Double shear specimen with bonded joints. All dimensions are in inches.

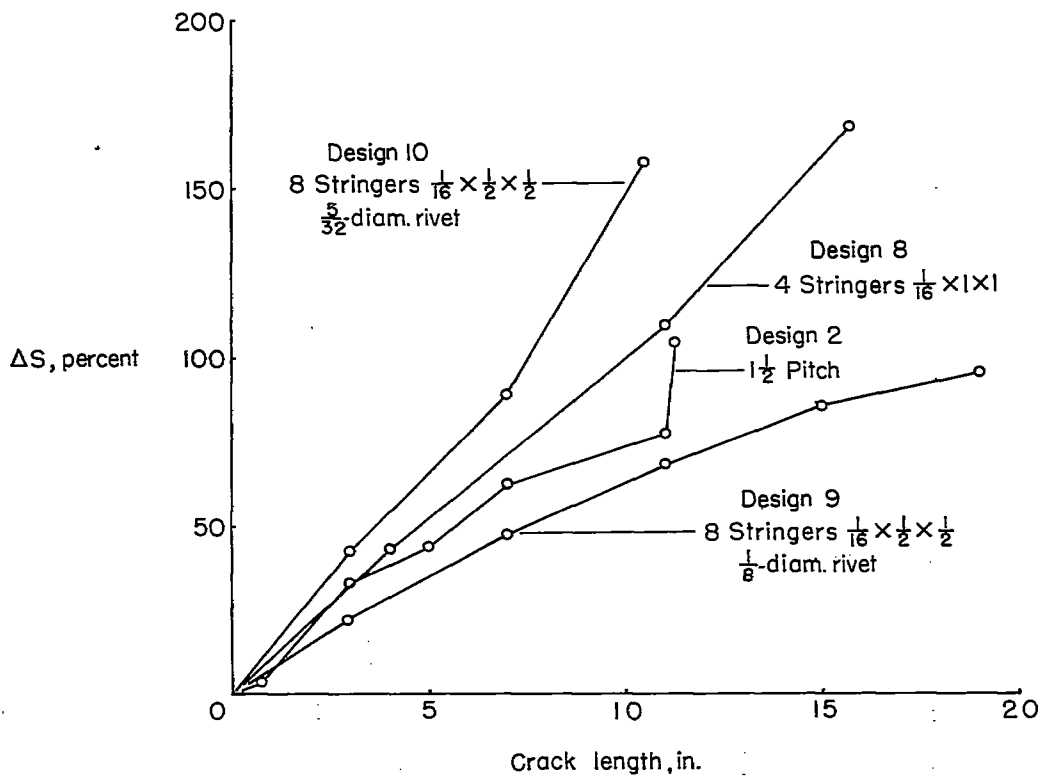
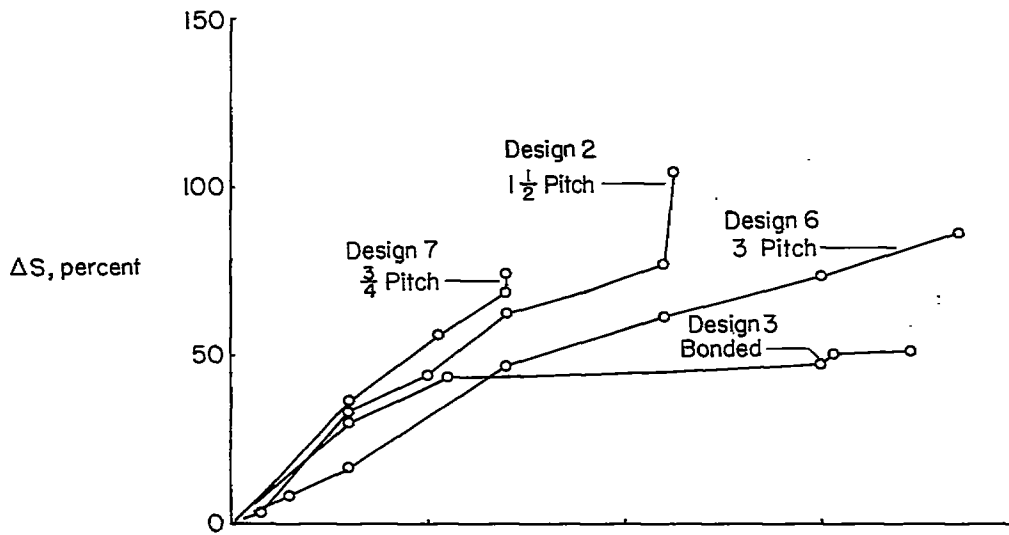


Figure 9.- Increase in stringer stress due to propagation of crack. All dimensions are in inches.